remote sensing

MDPI

Review

Challenges and Opportunities in Remote Sensing-Based Fuel Load Estimation for Wildfire Behavior and Management: A Comprehensive Review

Arnick Abdollahi [1,2,*] and Marta Yebra [2,3]

[1] Centre for Compassionate Conservation, TD School, University of Technology Sydney, Sydney, NSW 2007, Australia
[2] Fenner School of Environment & Society, College of Science, The Australian National University, Canberra, ACT 2601, Australia; marta.yebra@anu.edu.au
[3] School of Engineering, College of Engineering and Computing Science, The Australian National University, Canberra, ACT 2601, Australia
* Correspondence: arnick.abdollahi@uts.edu.au

Abstract: Fuel load is a crucial input in wildfire behavior models and a key parameter for the assessment of fire severity, fire flame length, and fuel consumption. Therefore, wildfire managers will benefit from accurate predictions of the spatiotemporal distribution of fuel load to inform strategic approaches to mitigate or prevent large-scale wildfires and respond to such incidents. Field surveys for fuel load assessment are labor-intensive, time-consuming, and as such, cannot be repeated frequently across large territories. On the contrary, remote-sensing sensors quantify fuel load in near-real time and at not only local but also regional or global scales. We reviewed the literature of the applications of remote sensing in fuel load estimation over a 12-year period, highlighting the capabilities and limitations of different remote-sensing sensors and technologies. While inherent technological constraints currently hinder optimal fuel load mapping using remote sensing, recent and anticipated developments in remote-sensing technology promise to enhance these capabilities significantly. The integration of remote-sensing technologies, along with derived products and advanced machine-learning algorithms, shows potential for enhancing fuel load predictions. Also, upcoming research initiatives aim to advance current methodologies by combining photogrammetry and uncrewed aerial vehicles (UAVs) to accurately map fuel loads at sub-meter scales. However, challenges persist in securing data for algorithm calibration and validation and in achieving the desired accuracies for surface fuels.

Keywords: fuel load estimate; forest fuels; fire behavior; fuel mapping; fire risk; remote sensing

Academic Editors: Angela Taboada and Paula García-Llamas

Received: 11 December 2024
Revised: 18 January 2025
Accepted: 24 January 2025
Published: 25 January 2025

Citation: Abdollahi, A.; Yebra, M. Challenges and Opportunities in Remote Sensing-Based Fuel Load Estimation for Wildfire Behavior and Management: A Comprehensive Review. *Remote Sens.* **2025**, *17*, 415. https://doi.org/10.3390/rs17030415

1. Introduction

Wildfires have the potential to significantly influence ecosystems, altering the composition, structure, and function of the vegetation by selectively favoring particular species and facilitating species introductions. However, they also play a critical role in maintaining the health and diversity of fire-prone ecosystems and altering biogeochemical processes like nutrient and carbon cycles and landscape patterns influenced by fire mosaics [1,2]. Additionally, some plants and animals are adapted to a regime of periodic fire, which reduces plant competition and diseases, benefiting the post-fire growth and development of vegetation. As a result, humanity has profited from fires for millennia through a variety of commodities and services, including hunting, tourism, pollination, food, and fiber [3].

However, due to global climate change and urbanization, the negative effects of wildfires have grown [4]. Associated with this is a commonly accepted notion that wildfires represent a form of natural hazard, posing risks to society, the economy, and the environment [5]. Since the early 1980s, there has been a statistically significant increase in wildfire frequency and the extent of the area burned, which has sparked increased interest in understanding wildfire hazards and behavior [6]. In addition, research on global meteorological patterns indicates that fire seasons are extending globally, and the severity of the fire weather is increasing [7]. Therefore, to effectively manage and provide early warning for wildfires, preventing or mitigating catastrophic fires, high-resolution and near-real-time assessments of wildfire danger become paramount [8]. Conventional fire danger assessment primarily relies on meteorological indicators like temperature, relative humidity, wind speed, and rainfall [9], which can be sourced globally from re-analysis data or locally from weather stations. However, understanding wildfire hazards and behavior requires incorporating fuel and topography factors, as outlined in the "fire environment triangle," [10] along with models like BehavePlus [11] and FARSITE [12] that rely on weather, topography, and detailed fuel inputs. Fuel-related factors, such as moisture content, spatial continuity, horizontal coverage, and load, play a crucial role in fire occurrence and behavior [13,14]. Accurate spatiotemporal predictions of these fuel properties can assist fire managers in reducing large-scale fire risks through prescribed burning and more effective fire spread prediction during active events [15,16].

However, while remote-sensing methodologies are well-established for determining fuel arrangement, composition, and moisture content [13,17,18], fully characterizing fire fuel load remains challenging. Fuel load refers to the amount of combustible material in a defined space, fuel type, and fuel layer [19]. Current techniques for fuel load characterization include destructive fuel inventories, fuel description systems, and fuel accumulation models. Destructive fuel inventories provide direct data but are labor-intensive and time-consuming, making universal field surveys impractical [20,21]. Fuel description systems, like those developed by Rothermel [22] or Ottmar, et al. [23], offer efficient alternatives for quantifying fuel loads by size-class categorizations related to fuel types. However, evidence suggests that using non-site-specific input data can bias fire simulations [24,25].

Fuel loads also vary across different fuel layers, encompassing not only surface fuel but also other fuel layers, exhibiting dynamic changes over time, and fuel load is a function of the balance between fuel accession and decomposition rates [26]. For example, surface litter fuel in forests accumulates when annual accession exceeds decomposition. After fires, fuel typically builds up quickly and steadily for a while, and then the accumulation rate gradually slows down to the equilibrium level [27]. Therefore, fuel loads can be estimated and predicted using fuel accumulation models, which have been implemented in land management decision-making [28]. A widely used exponential function describes surface litter fuel rapidly increasing to a steady state [27,29,30] using the following equation:

$$w_t = L/k\left(1 - e^{kt}\right) \quad (1)$$

where k is the decomposition constant, L denotes the accumulated surface litter fuel mass under steady-state conditions, and w_t is the surface litter fuel mass at time t (years since the last fire). The years since the last fire, the only independent factor that predicts fuel load growth within the general framework of the fuel accumulation model, cannot be used to assess the spatial variability in fuel load within vegetation burned at the same time. Also, another limitation aspect is the proportion of fuel consumed at the last fire, which will determine whether the accumulation has an intercept of zero fuel. Consequently, the manner in which fuel accumulates varies not only based on environmental factors, the type of vegetation species present, and the time since fire, but also the burned severity [31,32].

Instead of steady-state fuel accumulation models, field measurements, or tabular values, predictive modeling can estimate spatial variability in fuel load by incorporating explanatory factors like soil type, fuel type, and canopy density, making it particularly valuable in areas without a known fire history [33]. For example, Agee, et al. [26] found a polynomial relationship between the blue gum (*Eucalyptus globulus*) basal area and dry fuel weight, linking greater crown volume with higher surface litter fuel. Similarly, Gilroy and Tran [34] used multivariate regression to identify canopy cover, fuel depth, and years since the last fire as significant predictors, with average annual rainfall being less influential. They suggested that adding more factors could further enhance the model's accuracy.

Long-term and large-scale earth observation or remote-sensing technologies offer a promising avenue for systematic, efficient, and accurate quantification of fuel load for various fuel layers across different scales and fuel types [35–37]. This is particularly crucial in dynamic circumstances, caused by disturbances such as fires and storms and inter-annual variations in factors influencing fuel loads such as rainfall. Enabling the consistent availability of comprehensive and high-quality fuel maps over large regions via the remote sensing of fuel loads could potentially offer valuable support to fire management strategies.

In this study, we conducted a comprehensive review of how remote-sensing technology has been utilized to estimate fuel load from various fuel layers across diverse fuel types. Additionally, our focus extends to other fuel attributes that directly or indirectly influence fuel load. The prior examination in this field was undertaken by Gale, et al. [38] who conducted a comprehensive review encompassing various remote-sensing applications for diverse forest fire fuel characterizations. While Gale, et al. [38] provided a broad overview, outlining the array of remote-sensing data used for forest fire fuels, our review delves more deeply into the data sources and techniques utilized to connect remote-sensing data to fuel load estimation. We not only highlight their limitations but also elucidate how cutting-edge machine-learning techniques, such as convolutional neural networks (CNNs) or a fusion of radiative transfer models (RTMs) with deep learning (DL) models, effectively address the shortcomings of empirical techniques that rely on linear or nonlinear relationships between the remote-sensing data and ground-based fuel load measurements. Furthermore, we underscore recent advancements in remote-sensing technologies on both the regional and global scales, showcasing their ability to generate up-to-date and precise fuel load estimations. Our review encompassed peer-reviewed articles from scientific journals or conference proceedings in English from Web of Science and Google Scholar databases with complete text provided by the publisher, published from 2010 to 2022 inclusive, and focused on remote sensing-based estimation of fuel load from different fuel layers across various fuel types. Articles were excluded if the full text was not available from the publisher or if they were not written in English. Different keyword combinations with Boolean operators, such as "Fuel Load Mapping" OR "Fuel Load Prediction" AND "Remote Sensing", "Fuel Load Estimation" AND "Remote Sensing", and "Fuel Load Monitoring" AND "Satellite Images" were used to identify relevant articles. We structured our review by the type of remote-sensing sensor, encompassing passive, active, and integrated sensors. In doing so, we evaluated the merits and limitations of these techniques and provided valuable perspectives for future research in the domain of estimating fuel load.

2. Fuel Load Definition and Its Influence on Fire Behavior

Fuel consists of the physical characteristics of both dead and live fuel, playing a crucial role in wildfire occurrence, severity, and spread. In forest ecosystems, fuel layers are categorized into surface, understory (elevated and near-surface), and canopy fuel layers [29] (Figure 1), each with attributes like bulk density, height, and loading (Table 1). Among these, fuel load holds particular significance, representing the quantity of both dead

and live biomass available for combustion in terms of dry biomass per unit area [39]. Fuel load mapping has become a vital tool for fire management, aiding in prescribed burning, promoting biodiversity through pyrodiversity, prioritizing fire suppression, and aligning fire management with conservation goals [40].

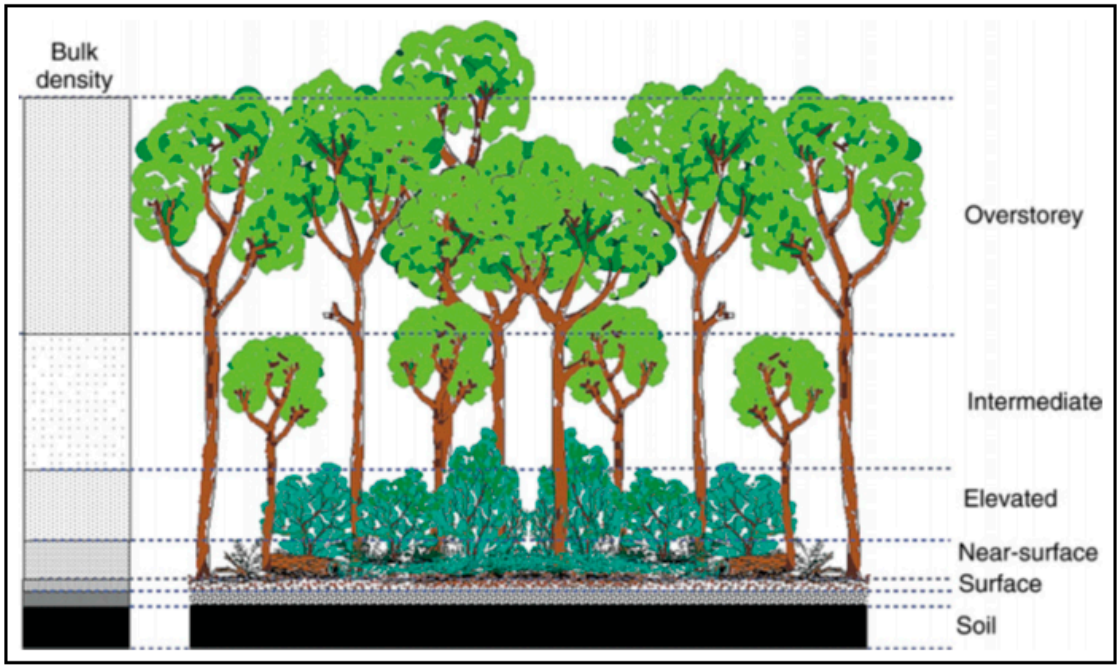

Figure 1. Distinct fuel layers within a dry eucalypt forest, with the grayscale on the left representing the relative bulk density of each layer [29]. Figure reproduced with permission.

Table 1. Various forest fuel attributes that play a crucial role in determining canopy, understory, and surface fuel load and its potential impact on fires.

Fuel Layer	Attribute	Definition	Role on Fire
Canopy layer	Canopy bulk density (CBD)	Amount of fuel in the canopy layer per unit of volume (kg/m^3).	Crown fire spread
	Canopy fuel load (CFL)	Amount of fuel in the canopy layer per area (kg/m^2).	
	Canopy height (CH)	The height of the tallest tree within the sampling area that impacts wind speed and trajectory.	
	Canopy base height (CBH)	Vertical distance between the surface and canopy fuel layers.	
Understory layer	Understory fuel load of shrubs, grasses, creepers, and small trees	Dry weight of combustible materials presents within this vegetation stratum in a given area (kg/m^2)	Fire transition from the surface to the canopy
Surface layer	Surface fuel load of all surface fuel elements (i.e., litter, logs, twigs, branches, herbaceous vegetation, and woody debris)	Dry weight of combustible materials found on or near the ground in a given area (kg/m^2) and are collectively determined by adding the estimated loads from all surface fuel layers.	Surface fire initiation and propagation

Crown fires are particularly concerning due to their severe, long-lasting impacts and difficulty in control, prompting fire managers to prioritize understanding crown fuel attributes. Key canopy attributes like canopy fuel load (CFL), canopy height (CH), canopy bulk density (CBD), and canopy base height (CBH) are widely acknowledged for their crucial role in determining crown fire propagation [41]. CFL, expressed in kg/m^2 or Mg/ha, represents the dry weight of canopy fuel per unit of area potentially available for ignition, influencing fire intensity and spread rate [41,42]. CBH, the vertical distance between the surface and the lowest canopy foliage, affects the likelihood of surface fires reaching the canopy, with a lower CBH increasing the overall fuel load and crown fire risk [43]. CBD quantifies the amount of fuel in the canopy layer per unit of volume (kg/m^3), influencing the speed at which fire can spread from one tree to another [44]. Higher CBD values indicate denser vegetation cover, leading to a more substantial accumulation of fuel load. CH not only affects wind trajectory but also reduces wind speed. The relation of CH with CFL is that taller canopies typically contain more biomass, contributing to a higher fuel load [41,42]. The significance of the canopy extends beyond influencing the spread and rate of fire through tree crowns. It also plays a crucial role in determining the type, volume, and distribution of surface fuel via litterfall which is also another important factor in wildfire behavior [41].

The understory fuel layers, consisting of shrubs, grasses, creepers, and small trees, play a critical role in wildfire behavior and spread. Shrubs can act as ladder fuels, enabling fires to climb from the surface to the canopy, while grasses, as fine fuels, ignite easily and rapidly spread fire. During dry periods, these understory fuels become highly flammable, increasing fire intensity and the likelihood of transitioning to crown fires. Understanding the composition and condition of understory fuels is vital for effective wildfire management and mitigation strategies [45,46].

Surface fuels are regarded as the most complex fuel types to manage in the context of wildfire. Most fire behavior prediction models, including BEHAVE, FlamMap, and FARSITE require a precise physical description of this fuel layer [12,47]. This description involves providing a detailed and quantifiable representation of the properties and characteristics encompassing factors such as fuel type, size, arrangement, moisture content, bulk density, and other relevant attributes that collectively define the composition and structure of surface fuels present within a given area [12,47].

Surface fuels, comprising dead and live biomass (i.e., litter, logs, twigs, branches, herbaceous vegetation, and woody debris), are crucial for the initiation and spread of surface fires [39,46]. Dead fuels play a pivotal role in wildfire prediction, influencing vegetation arrangement and flammability. Surface fuel load, measured as the dry weight of the surface fuel layer per unit area (kg/m^2), is a key parameter in fire behavior models, affecting fire spread rate and fire-line intensity [48]. The load of specific surface fuel types is critical because different fuel types affect fire behavior models differently. To use fire behavior models and danger systems effectively, the physical parameters of each fuel type, such as load, must be quantified numerically [49]. Fine woody debris (FWD) with diameters less than 0.64 cm and litter are conspicuous examples of critical surface fuel loads, as they dry quickly and ignite easily, unlike larger woody fuels, which are more resistant to drying and ignition [50]. Downed woody debris (DWD), comprising dead and fallen materials (e.g., twigs, branches, stems, and trunks), is categorized into four time-lag classes—1 h (<0.64 cm diameter), 10 h (0.65–2.54 cm diameter), 100 h (2.55–7.6 cm diameter), and 1000 h (>7.6 cm diameter)—based on their moisture equilibrium rates, reflecting their varying roles in fire behavior [51].

3. Remote-Sensing Techniques for Fuel Load Mapping

Remote sensing provides a wide array of sensors and methodologies for mapping fuel loads. In this section, we present various remote-sensing techniques for fuel load and other related fuel attributes mapping, categorized according to the type of sensor employed. These categories encompass passive sensors, active sensors, or combined approaches.

3.1. Passive Sensors

Passive sensors are remote-sensing devices that capture electromagnetic radiation emitted or reflected by objects without emitting their own energy. Passive optical sensors, such as those onboard of Landsat, Sentinel, Terra/Aqua, and QuickBird, capture and measure electromagnetic radiation in the visible and infrared parts of the electromagnetic spectrum and have commonly been employed to assess fuel attributes, including fuel load. Generally, fuel load models are established through the calibration of empirical relationships between spectral data acquired by these sensors and on-ground observations [52]. Multispectral optical remote-sensing captures the spectral reflectance of the canopy, which can reveal both the geometric characteristics of standing woody components and the biochemical traits of leaves [53]. Numerous research endeavors have leveraged optical imaging to establish predictive techniques that portray the spatial variances of fuel load (Table 2).

Using basic spectral analysis, Jin and Chen [54] demonstrated the correlation between fuel loads and stand characteristics such as mean diameter at breast height (DBH) and stand height using multispectral and low-resolution Landsat Thematic Mapper™ and high-spatial-resolution (<5 m) QuickBird imagery in northeastern China. They found stand attributes to be correlated and intertwined with fluctuations in fuel load levels. The QuickBird imagery provided accurate estimations of fuel loads and outperformed the lower-resolution Landsat TM imagery. In many cases, QuickBird estimations were as good as those based on surveyed stand characteristics at 70 plots, particularly for fine and total dead fuel loads. However, the estimation of coarse fuel loads was less accurate with either of these two satellite images due to their weaker association with stand characteristics. Building on Jin and Chen's work on basic spectral analysis, the work in [40] introduced a more sophisticated approach using partial unmixing techniques. They mapped variations in fuel loads over wide areas of the Brazilian savanna using Sentinel-2 and Landsat 8 data and a partial unmixing technique called mixture tuned matched filtering (MTMF). The study found a strong correlation (R^2 = 0.81) through linear regression analysis between in situ data and matched filter scores for dry vegetation, indicating the method's effectiveness in mapping fuel loads variations. Arellano-Pérez, et al. [55] further advanced fuel load estimation by incorporating various vegetation indices such as the enhanced vegetation index (EVI), soil adjusted vegetation index (SAVI), modified soil adjusted vegetation index (MSAVI), normalized difference vegetation index (NDVI), and red edge normalized difference vegetation (RENDVI) along with Sentinel-2A bands in the modeling as explanatory variables. They performed random forest (RF) and multivariate adaptive regression splines (MARS) techniques to characterize and estimate canopy and surface fuel structure and load-related attributes such as CBD, CBH, and surface fuel load. The estimated fuel loads for each surface fuel layer (e.g., duff, litter, DWD, and shrubs and herbaceous layers) were added up to determine the total surface fuel load. The results underscore that the integration of medium-resolution imagery with machine-learning techniques can contribute significant insights into the surface and canopy fuel attributes on a larger scale. This combination enables the classification of factors such as crown fire potential and the potential wildfire type, thereby enhancing the understanding of fire behavior and its potential impacts.

Quan, et al. [14] marked a significant leap by combining machine learning with radiative transfer models (RTM). They used this combination to retrieve the foliage fuel load (FFL) from Landsat 7 Enhanced Thematic Mapper Plus (ETM+) and 8 Operational Land Imager (OLI) data. RTMs offer a valuable methodology for extracting biophysical and biochemical parameters from remote-sensing data. These models are constructed on the foundation of physical principles that establish clear connections between the properties of canopies or leaves and the resulting reflectance. Consequently, RTM-based techniques possess a distinct advantage of reproducibility, making them applicable to diverse locations and satellite sensors. This adaptability allows for the estimation of relevant variables of interest across a spectrum ranging from local to global scales. They employed the PROSAIL RTM to generate a look-up table (LUT) of simulated canopy reflectance spectra for various biophysical parameters, including FFL. From these simulated spectra, they calculated several vegetation indices (VIs) sensitive to fuels, including the NDVI, two normalized difference infrared indices (NDII6 and NDII7), moisture stress index (MSI), global vegetation moisture index (GVMI), EVI, visible atmospherically resistant index (VARI), global environmental monitoring index (GEMI), and greenness index (Gratio). These VIs were then used as input features to train three machine-learning models: RF, Support Vector Machine (SVM), and Multilayer Perceptron (MLP). The machine-learning algorithms were trained to predict FFL based on the relationships established in the RTM-generated LUT. This approach allowed the models to learn the complex relationships between the VIs and FFL as simulated by the RTM. The trained models were then applied to real satellite data to retrieve the FFL. Additionally, MODIS reflectance products were used in conjunction with the RTM models to further refine and validate the FFL retrieval process, integrating multiple data sources into the assessment. The accuracy assessment of FFL estimates was carried out within a forest located in southwestern China, encompassing two fire incidents in 2014 and 2020. The resulting MLP model, with an R^2 value of 0.77 between observed and retrieved predictions, demonstrated a higher performance compared to the other methods. This finding underscores the significance of combining machine learning with RTM for FFL estimates derived from remote sensing.

Oliveira, et al. [56] developed temporal dynamics and a biome-specific approach focused on estimating fuel load dynamics in Brazilian grasslands and savannas, using an RGB composite of three Landsat 8 bands, namely red, near-infrared, and short wavelength infrared with historical burned areas. The correlation between fuel loads and the remote-sensing data used varies from 0.27 to 0.88 for different fuel types (with an average correlation of R^2 = 0.61 and a standard deviation of 0.18) across the Cerrado region. Wells, et al. [57] further refined this approach by estimating yearly fine-fuel loads from 2015 to 2020 in semi-arid grasslands using Sentinel-2A imagery, in situ fuel loads, and machine learning. They included 11 of the 13 total Sentinel-2A bands available for each image during the periods of vegetation dormancy and vegetation peak greenness in the analysis. The fine-fuel model correlated well with on-site validation in the initial (R^2 = 0.52, Root Mean Square Error (RMSE) = 218 kg/ha) and final (R^2 = 0.63, RMSE = 196 kg/ha) years of the 6-year study. By providing a more advanced validated model that effectively captures the complexities of fine-fuel dynamics, this study highlights the potential of integrating remote-sensing data, in situ fuel loads, and machine learning. Chaivaranont [58] introduced an innovative temporal dynamics approach using vegetation optical depth (VOD) derived from the Advanced Microwave Scanning Radiometer—Earth observing system (AMSR-E) to estimate the grasslands fuel load. More specifically, the author converted the annual mean VOD to gridded annual aboveground biomass (AGB) serving as a proxy for fuel load. This satellite-based ABG product was then regressed with fuel load measures from the ground according to Australian bioregions. Additionally, a vegetation structure

dataset was used to assess the utility of the AGB dataset as a proxy for evaluating the estimated fuel load data. The outcomes of this evaluation indicated that nationwide AGB estimates obtained through VOD could approximately depict the characteristics of vegetation structure, achieving a significant relationship with an R^2 of 0.82. This observation inferred that estimates of fuel load derived from AGB were in alignment with the characteristics of vegetation cover. Consequently, the model was able to reasonably predict fuel load quantities across Australia, with higher fuel loads correlating with taller and denser vegetation covers.

Overall, the utilization of optical data and associated methodologies has proven effective in estimating fuel loads within the tree canopy. However, their precision somewhat diminishes when assessing surface fuel loads due to limitations in optical sensors to effectively penetrate dense canopies [55]. To bolster the accuracy of assessments, incorporating stand-related factors such as stand age, closure, height, and basal area have shown significant correlations and enhancements in predictions of both canopy and surface fuel loads [59]. Nonetheless, the effort to predict these stand-related variables from optical remotely sensed data introduces inaccuracies into the estimation process due to their inherent limitations, such as the inability to determine whether the detected signal comes from the canopy, understory, or ground, which subsequently affects the accuracy of stand-related variable estimations. To counter this constraint and refine the precision of fuel load estimation, the integration of active sensors like LiDAR has been proposed [60]. LiDAR can furnish intricate insights into canopy structure, height, and biomass metrics. The inclusion of a LiDAR remote-sensing approach facilitates a more precise evaluation of height and biomass-related parameters, ultimately culminating in heightened accuracy when estimating both canopy and surface fuel loads.

Table 2. Optical and microwave remote-sensing data and their use in modeling fuel load parameters and other key variables crucial in shaping fuel load.

Data Source	Parameters	Definition	Estimated Variables	Citation
Landsat	Band 1	Blue	Foliage fuel load (FFL)	[14,40,54]
	Band 2	Green		
	Band 3	Red		
	Band 4	Near infrared (NIR)		
	Band 5	SWIR1		
	Band 7	SWIR2		
	EVI	Enhanced vegetation index		
	NDII6/NDII7	Normalized difference infrared indices		
	GEMI	Global environmental monitoring index	Grassland and savanna fuel load	[56]
	GVMI	Global vegetation moisture index		
	NDVI	Normalized difference vegetation index		
	VARI	Visible atmospheric resistant index		
	MSI	Moisture stress index		
	G_{ratio}	Greenness index		

Table 2. *Cont.*

Data Source	Parameters	Definition	Estimated Variables	Citation
Sentinel-2	Band 2	Blue	Surface fuel load (SFL) for each surface fuel layer (e.g., duff, litter, DWD, and shrubs and herbaceous layers) Fuel strata gap (FSG), canopy base height (CBH), canopy bulk density (CBD) Grassland fuel load	[55] [57]
	Band 3	Green		
	Band 4	Red		
	Band 5	Red Edge		
	Band 6	Red Edge		
	Band 7	Red Edge		
	Band 8	Near Infrared (NIR)		
	Band 8A	Near Infrared (NIR)		
	Band 11	SWIR1		
	Band 12	SWIR2		
	SAVI	Soil adjusted vegetation index		
	MSAVI	Modified soil adjusted vegetation index		
	EVI	Enhanced vegetation index		
	NDVI	Normalized difference vegetation index		
MODIS	Bands	Reflectance products	Foliage fuel load (FFL)	[14]
AMSR-E	VOD	Vegetation optical depth	Grassland fuel load	[58]
QuickBird	B1	Blue	Diameter at breast height (DBH), stand height, fine, coarse and total dead fuel loads	[54]
	B2	Green		
	B3	Red		
	B4	Near Infrared (NIR)		

3.2. Active Sensors

Radio Detecting and Ranging (RADAR) is an active remote-sensing technology that uses polarimetric information and it is unaffected by weather conditions. It has been widely used to observe various Earth surface variables such as soil and fuel moisture contents [61,62]. RADAR, particularly those with long wavelengths, have shown immense potential for estimating fuel load such as CFL, foliage biomass, stem fuel load (SFL), branch fuel load (BFL), and FFL [63,64]. RADAR sensors transmit different wavelength bands (X-, C-, L-, and P-band), which have varying levels of penetration into vegetation layers. For example, the L- and P-band signals, which have a longer wavelength, interact with thick trunks and branches, making them better suited for fuel load mapping, whereas the C-band has shorter wavelengths which can penetrate foliage but will be scattered by small branches [65,66]. Airborne L- and P-bands' horizontal–vertical (HV) polarizations were used by Saatchi, et al. [63] to determine the CFL empirically. The fuel characteristics derived from RADAR data showed a notable alignment with the fuel measurements taken in the field, resulting in coefficients of determination of $R^2 = 0.85$ for the canopy fuel load and $R^2 = 0.78$ for the foliage biomass. Airborne RADAR's ability to monitor fuel load is constrained by its high cost, while spaceborne RADAR provides a more economical option.

LiDAR is another active sensor that operates by emitting a laser beam and receiving backscattered or reflected light from the target [67]. In comparison to other remote-sensing data, LiDAR can give three-dimensional information on the structure of the forest and the spatial characteristics of the depth and coverage of surface fuel, canopy density, and topography [68]. Numerous research efforts have utilized active remote-sensing data, including LiDAR and RADAR, to develop predictive techniques that estimate spatial variations in fuel load (Table 3).

Some research focused on the potential of the airborne LiDAR system (ALS) for regional-scale assessments. Skowronski, et al. [59] used ALS data, calibrated with field plots and allometric equations, to estimate canopy fuel loading. The LiDAR datasets were applied to predict CBD and CFW in wildfire-prone areas of the New Jersey Pinelands. Additionally, LiDAR-derived height profiles were created in 1 m layers and regressed against CBD estimates from field plots to assess three-dimensional canopy fuel loading. Their findings indicated that single-beam LiDAR has potential for estimating regional-scale canopy fuel loading. However, the weakest relationships were observed in the mid-canopy, where the fuel loading variability and average values were highest. Hermosilla, et al. [24] further explored the capabilities of full-waveform LiDAR-derived metrics to assess forest canopy parameters (e.g., CH, CBH, CBD, and CFL) and structural fuel parameters (e.g., stand density index and volume, basal area, and aboveground biomass) in north-west Oregon (United States). By estimating parameters such as CH and stand density index, their study demonstrated the potential of full-waveform airborne LiDAR to describe various fuel parameters. The results demonstrated strong explanatory power for aboveground biomass modeling (R^2 = 0.84), CH (R^2 = 0.79), CBH (R^2 = 0.78), and CFL (R^2 = 0.79). Cameron, et al. [69] also explored the fuel characteristics of black spruce stands such as CFL, CH, CBH, and CBD in Alberta, Canada, using ALS data and field measurements. Least absolute shrinkage and selection operator (lasso) regression models demonstrated statistically significant connections between ALS data and the forest metrics of interest. These relationships were particularly strong, with an R^2 value of 0.81 for all metrics except for CBH, which had an R^2 value of 0.63. Stefanidou, et al. [70] further explored the capability of discrete-return multispectral airborne LiDAR data with structural and intensity information to reliably estimate surface fuel load, including litter, downed woody debris, forbs, and grass and shrubs in a dense coniferous forest based on derived height and intensity distribution metrics. The linear regression analysis method and leave-one-out cross-validation was employed to evaluate predictive models utilizing different sets of predictor variables, revealing that models combining structural and intensity metrics outperformed those using individual metrics, with a notable explained variance (R^2) ranging from 0.59 to 0.70. These findings highlight the significance of both structural and intensity variables obtained from multispectral LiDAR data for surface fuel load estimation.

Other approaches to improving fuel load estimation have focused on integrating various datasets, including field surveys, time-since-fire metrics, topographic elements, and fuel characteristic classification systems, with ALS measurements. These efforts have aimed to address challenges in capturing spatial variability and improving the accuracy of fuel load modeling in diverse landscapes. Price and Gordon [71] conducted research on postfire mid-story and canopy fuel accumulation, focusing on dry sclerophyll forests in the Sydney Basin, Australia. They integrated airborne LiDAR data with field surveys to assess the fire hazard, contributing to a better understanding of fuel dynamics at fine geographical scales. They conducted an examination of how effectively time-since-fire serves as an indicator for vegetation cover and accumulation, with these parameters being utilized to estimate fuel load. Their specific focus was on the vegetation strata (0.5–4 m, 4–15 m, >15 m) crucial for the spread of crown fires, and they quantified the percentage of fuel cover and accumulation in three distinct vegetation height categories: elevated fuels (0.5–4 m), lower canopy fuels (4–15 m), and upper canopy fuels (15–45 m). Their findings revealed that time-since-fire is an unreliable predictor for the accumulation of mid-story and canopy fuels, particularly in capturing spatial variability. This result underscores the limitations of using temporal proxies for fuel load modeling in heterogeneous landscapes, highlighting the need for methodologies that account for finer-scale variability. Similarly, Lin, et al. [72] suggested a methodology for producing surface fuel load maps (fine and total surface fuel loads)

by combining multiple linear regression methods, airborne LiDAR, and topographic data with in situ fuel inventory data and classified fuel models (forest types). The synergy of topographic elements, such as slope and aspect, as explanatory variables, along with their interactions with fuel types (pine, non-pine conifer, broadleaf, and conifer–broadleaf mix) effectively characterized variations in surface fuel loads across diverse terrain morphology such as different altitudes and different aspects of the slope. By using cross-validation, the estimation of total and fine surface fuel load maps for the study area yield RMSE values of 3.476 tons/ha and 3.384 tons/ha, respectively. This approach demonstrated its effectiveness in addressing the complexities of undulating terrain and inaccessible regions, underscoring the importance of integrating terrain and vegetation characteristics into fuel load estimation models. Building on the theme of integration, McCarley, et al. [73] utilized multitemporal airborne laser scanning data along with the fuel characteristic classification system (FCCS), a widely-used fuel classification system that was designed and applied across all ecosystems in the United States, adapted for use in LANDFIRE (LF), to estimate the total pre-fire fuel load. Pre-fire ALS data for the Tepee Fire consisted of two collections from 2010 and 2011, whereas the pre-fire ALS data for the Keithly Fire were gathered in 2017. This encompassed the sum of individual fuelbed categories, including duff, litter, downed woody debris, herbaceous vegetation, and shrubs. The results indicated that the LF FCCS approach produced higher estimates of pre-fire fuel loads and fuel consumption than the ALS approach. However, the coarse resolution of FCCS data failed to capture the fine-scale heterogeneity effectively represented by ALS. This finding highlights the potential of integrating coarse FCCS data with finer-scale ALS measurements to improve finer-scale spatial variability and accuracy in fuel load quantification.

While ALS proved effective in estimating spatial variations in fuel load, some studies revealed limitations. González-Ferreiro, et al. [74] utilized low-density (up to 0.5 pulses m-2) airborne laser scanning (ALS) data and Spanish national forest inventory data to predict the vertical distribution of canopy fuel variables for different pine species in Galicia, Spain. Their research provided estimates of canopy fuel variables, namely CFL, CBH, and CBD, specific to the maritime pine and radiata pine stands. The canopy fuel load derived from field measurements accounted for 84% of the variability in maritime pine and 86% in radiata pine, while the canopy fuel load based on ALS metrics explained 52% for maritime pine and 49% for radiata pine, suggesting that low-density data might not be sufficient for highly precise estimations of canopy fuel load. To address the limitations of ALS, terrestrial laser scanning (TLS) has emerged as a valuable complement, offering high-density, high-resolution data well-suited for detailed assessments of vegetation layers in specific areas. Alonso-Rego, et al. [20] examined TLS's potential for estimating shrub, litter, and live/dead fuel loads in Galicia, Spain. Two methods for estimating fuel loads and live/dead fractions from TLS data were compared: (i) Indirect estimation (IE) involved a two-step process. Initially, three equations were fitted to estimate shrub height, shrub cover, and litter depth from TLS data. These estimates were then used as inputs for existing species-specific fuel load equations, segmented by size fractions; and (ii) direct estimation (DE) consisted of fitting seven equations, one for each fuel fraction, to directly estimate fuel loads for each size category using TLS data. Overall, the direct method showed a better performance, explaining over 80% of the variability for fuel load for all fuel layers except litter loads.

Recognizing that ALS and TLS each bring unique strengths and limitations, Chen, et al. [68] combined these data sources to improve surface fuel load modeling in the Upper Yarra Reservoir Park, Victoria, Australia. Their model, which incorporated fuel type, elevation, and canopy density as predictors, demonstrated an R^2 of 0.89, significantly outperforming models using ALS alone, such as McArthur's (R^2 = 0.61) and Gilroy and

Tran's (R^2 = 0.69). The high accuracy of the combined model underscores the value of integrating ALS with TLS to enhance predictive power, especially when using multiple regression analysis. Expanding on this integration, Alonso-Rego, et al. [75] explored how combining TLS and low-density ALS with machine learning could improve fuel variable estimates, specifically canopy and surface metrics in pure stands of Pinus pinaster and Pinus radiata. They applied three machine-learning models—SVM, RF, and multivariate adaptive regression splines (MARS)—to estimate variables such as CBD, CFL, CBH, stand mean height (SMH), fuel strata gap (FSG), and surface fuel loads. TLS data proved more effective for inner canopy and understory assessments, though challenges remained in capturing upper canopy details due to mid-canopy foliage obstruction. Their findings suggested that combining ALS and TLS metrics with machine learning provides a promising alternative to field surveys, offering accurate surface/canopy fuel load estimates on a broader scale.

The studies mentioned above showed that metrics derived from airborne and terrestrial LiDAR systems have the potential to estimate fuel load and other related fuel attributes. However, it is crucial to recognize that each system comes with its own set of trade-offs, and these trade-offs can influence the accuracy of the predictive models. The terrestrial system provides high-resolution data on the characteristics of understory vegetation and canopy structural diversity by capturing the vegetation structure from below the canopy from ground. However, due to mid-canopy foliage occlusion, terrestrial measurements are less reliable for calculating upper canopy parameters and may not fully characterize the distribution and density of vegetation throughout the canopy. This incomplete representation can lead to inaccuracies in estimating fuel loads, particularly when considering the contribution of vegetation in the upper canopy to overall fuel load or canopy fuel load [76]. Conversely, the vegetation structure is captured by the airborne system from above. As a result, it provides a higher level of information in the top canopy and decreases accuracy in portraying canopy and subcanopy properties as canopy depth increases, particularly for species with dense canopies. This limitation can impact the precision of fuel load estimations, particularly in areas with complex canopy structures where dense vegetation might obscure underlying layers [75]. The models' overall accuracy of fuel load estimates can be improved as a result of combining the benefits of both airborne and terrestrial LiDAR systems by incorporating both sets of metrics as predictor parameters [68]. However, both terrestrial and airborne LiDAR have limitations when it comes to fuel load mapping at continental and global scales. Thus, the capability of spaceborne LiDAR sensors such as Global Ecosystem Dynamics Investigation (GEDI) or ICESat/GLAS for predicting large-scale fuel load and other vegetation structural measures will aid in tackling the limitations faced by airborne and terrestrial LiDAR systems when estimating fuel characteristics across wider geographic areas, though space-borne data with lower spatial resolution may even have an aggravated problem of canopy occlusion than airborne lidar [77,78].

Table 3. Active sensors-derived metrics for estimating fuel load metrics and other key variables crucial in shaping fuel load.

Data	Data Characteristic	Metrics	Definition	Estimated Variables	Citation
LiDAR	Height	H_{10}, H_{25}, H_{50}, H_{75}, H_{90}, H_{95}, H_{99}	Height percentiles	Canopy fuels: canopy base height (CBH), canopy fuel load (CFL), canopy bulk density (CBD), canopy height (CH) Stand variables: tree height, diameter at breast height (DBH), basal area, quadratic mean diameter, volume, stand density index, aboveground biomass Surface fuels: total surface fuel load (TSFL), surface fuel types' load (SFTL)	[24,70,75,79]
		Mean_h	Mean height		
		Std_h	Standard deviation		
		CD_h	Canopy depth		
		Kurt_h	Kurtosis		
		Skew_h	Skewness		
		CC_h	Canopy cover		
		CV_h	Coefficient of variation		
	Intensity	I_{10}, I_{25}, I_{50}, I_{75}, I_{90}, I_{95}, I_{99}	Intensity percentiles		
		CC_i	Canopy cover		
		Kurt_i	Kurtosis		
		Skew_i	Skewness		
		Range_i	Range of intensities		
		CV_i	Coefficient of variation		
		Std_i	Standard deviation intensity		
		Mean_i	Mean intensity		
		Max_i	Maximum intensity		
RADAR	Frequency	L- and P-band	Radio frequency at which the system emits and receives electromagnetic waves	Canopy fuel weight (CFW), canopy bulk density (CBD), foliage biomass (FB)	[63,65]
	Polarization	HV, HH, VV	Orientation of the oscillations of the electric field component		

3.3. Combined Remote-Sensing Sensors

Several studies have explored the potential of combining passive and active sensors to estimate fuel metrics relevant to retrieve fuel loads, particularly in the last decade (Table 4). This approach provides a more comprehensive picture of the fuel characteristics in an area compared to relying on a single sensor type.

Early studies, like the one by Erdody and Moskal [80], laid the groundwork by demonstrating the value of combining LiDAR data, which provides detailed 3D information about vegetation structure, with passive imagery like color near-infrared aerial photographs to quantify CFL and other various canopy fuel parameters in shaping fuel load, including CBD, CBH, and CH. The results indicated that LiDAR contributed to enhancing the precision and accuracy of canopy fuel measurements when compared to relaying on passive imagery alone. Incorporating imagery with LIDAR improved the R^2 value from 0.94 to 0.96, 0.78 to 0.84, 0.83 to 0.88, and 0.88 to 0.91 for CH, CBH, CBD, and CFL, respectively. Building upon this foundation, subsequent studies incorporated high-resolution imagery and advanced data analysis techniques. Skowronski, et al. [81] incorporated high-resolution 0.3 m multispectral orthophoto imagery and a technique called object-oriented fuel categorization

alongside ALS data to quantify canopy fuel load and distribution in the wildland–urban interface. Their study confirmed the link between the type of forest cover observed in the high-resolution imagery and the fuel load derived from the LiDAR data with a statistically significant linear relationship of $R^2 = 0.66$.

Researchers have also explored the use of multi-temporal remote-sensing data across fire events. García, et al. [79] introduced a method that combined pre-fire data from Landsat OLI satellites with post-fire airborne LiDAR data to estimate pre-fire canopy fuel characteristics such as CBD, canopy cover, and CFL. CFL and CBD were first estimated using LiDAR data with derived height and intensity information. Subsequently, LiDAR-based canopy fuel characteristics were extrapolated over the entire area using the spectral bands (B2-B7) of Landsat OLI data. In addition, the authors also incorporated various other factors as proxies of fuel load estimation such as NDII, VARI, EVI, NDVI, and the tasseled cap transformation (TCT). This approach yielded notable results, with R^2 values of 0.8, 0.79, and 0.64 between observed and modeled CFL, canopy cover, and CBD, respectively, demonstrating a more comprehensive approach for fuel characterization by incorporating data from both pre- and post-fire scenarios.

The focus of research has also shifted towards estimating specific fuel components and emphasizing the importance of selecting appropriate data sources tailored to the targeted fuel load component. Li, et al. [82] combined Sentinel-2 optical and Sentinel-1 SAR satellite data with an RF regression model to specifically assess dead fuel load, including 1 h, 10 h, 100 h fuels, litter, and their total. This study was conducted in the southwestern region of Sichuan, China. Sentinel-1's dual-polarization capabilities proved particularly valuable, as they allowed penetration of the canopy to capture underlying conditions, which was essential for accurately estimating the dead fuel load. The findings indicated that optical (sentinel-2) and SAR (Sentinel-1) data are a better indicator for measuring the 1 h ($R^2 = 0.57$) and total dead fuel load, comprising 1 h, 10 h, 100 h, and litter ($R^2 = 0.59$). In contrast, the predictive capability of optical and SAR data was relatively less robust for 10 h ($R^2 = 0.41$), 100 h ($R^2 = 0.40$), and litter ($R^2 = 0.29$). This study highlighted the effectiveness of combining optical and SAR remote-sensing data sources to target specific fuel components such as the 1 h and total dead fuel load, enabling a more focused approach to fuel load assessment. Li, et al. [64] compared the performance of combining optical data (Landsat TM+) with synthetic aperture RADAR (ALOS PALSAR) data with the L-band for estimating different fuel loads such as the foliage fuel load (FFL), branch fuel load (BFL), and stem fuel load (SFL). Optical data yielded the most accurate results for FFL estimation ($R^2 = 0.66$), followed by a moderate performance for both BFL ($R^2 = 0.56$) and SFL ($R^2 = 0.37$) estimation. Notably, further enhancements were observed in estimating SFL, BFL, and FFL when integrating optical and SAR data ($R^2 = 0.76$, 0.81, and 0.82, respectively) compared to using just one type of data. This emphasizes the need for thoughtful data selection based on the specific fuel component of interest.

The latest advancements involved using machine-learning algorithms and placing a strong emphasis on multi-sensing data composition. D'Este, et al. [83] employed machine-learning techniques like SVM, RF, and multiple linear regression (MLR) to estimate the fine dead fuel load (referring to 1 h time-lag fuels with a diameter of 0–0.65 cm) using a combination of LiDAR, Sentinel-1, and Sentinel-2 data. Sentinel-2 data were used to calculate NDVI, NDWI, and NDMI, whereas Sentinel-1 data were utilized with both VV (vertical transmit–vertical receive) and VH (vertical transmit–horizontal receive) polarizations. In addition, LiDAR data calculated the canopy height model (CHM) based on a digital terrain model (DTM) and digital surface model (DSM), facilitating the extraction of vegetation and canopy cover information. The findings indicated that RF exhibited a better predictive capability with an R^2 value of 0.50 compared to SVM and MLR, which showed a

similar performance with R^2 values of 0.39 and 0.40, respectively. Also, the authors found that CHM and canopy cover, derived from LiDAR data, were more important in fuel load estimation compared to optical and RADAR variables like vegetation indices or polarizations. Notably, the outcomes underscored a positive correlation between the presence of the tree components (e.g., cover and height) and the 1 h fuel load. On the contrary, geomorphological variables demonstrated comparatively weaker predictive capabilities. This trend underscores the increasing role of sophisticated algorithms and diverse data sources in enhancing fuel load assessment accuracy.

As demonstrated by the studies mentioned earlier, passive and active remote-sensing data each offer unique strengths in estimating fuel load. While passive data are sensitive to biochemical attributes, active data provides critical insights into the vertical structure and distribution of forest fuels, encompassing surface fuels. Combining these complementary data types can enhance the accuracy of fuel load predictions by leveraging the strengths of each approach [82].

Table 4. Overview of combined remote-sensing data used for fuel load estimation and other essential variables pivotal in determining fuel load characteristics.

Data Sources	Parameters	Definition	Estimated Variables	Citation
Aerial color infrared Imagery	Bands 1–3	Green, red, NIR	ACF, CBD, CBH, and CH	[80]
	NDVI	Normalized difference vegetation index		
LiDAR	Height information	Height distribution of LiDAR returns		
Landsat OLI	Bands 2–7	Blue-SWIR2	CBD, CC, CFL	[79]
	NDII	Normalized difference infrared indices		
	VARI	Visible atmospheric resistant index		
	EVI	Enhanced vegetation index		
	NDVI	Normalized difference vegetation index		
	TCT	Tasseled cap transformation		
LiDAR	Height	Height distribution of canopy returns		
	Intensity information	Intensity values of each LiDAR return		
Sentinel-1	VH	VH polarization	Dead fuel load (DFL)	[82]
	VV	VV polarization		
Sentinel-2	Bands 2–12	Blue-SWIR2		
Landsat ETM+	Bands 1–7	Blue-SWIR2	FFL, BFL, and SFL	[64]
ALOS PALSAR	HH	HH channel		
	HV	HV channel		
LiDAR	CHM	Canopy height model	Fine dead fuel load (FDFL)	[83]
Sentinel-1	VH	VH polarization		
	VV	VV polarization		
Sentinel-2	Bands 2–12	Blue- SWIR1		
	NDVI	Normalized difference vegetation index		
	NDWI	Normalized difference water index		
	NDMI	Normalized difference moisture index		

4. Challenges in Estimating Fuel Load with Remote-Sensing Data

In this section, we explore the difficulties faced when using remote-sensing data to estimate fuel load. These challenges are crucial because they affect how accurately we can predict fuel load and fall into two main categories: how we build our models to make these estimates, which is determined by the specific technique used to link remote-sensing data to fuel load (methodological challenges); and the quality and capability of the specific sensor or remote-sensing data used to estimate fuel load for various fuel layers across diverse fuel types (sensor data challenges).

4.1. Methodological Challenges

Remote sensing-based fuel load prediction often involves the application of empirical techniques that rely on linear or nonlinear relationships between the remote-sensing data and ground-based fuel load measurements. These empirical methods are straightforward to calibrate, require less computational complexity, and therefore have been broadly utilized [38,40]. However, these techniques generally lack reproducibility, as they rely on site-dependent and sensor-specific relationships, making them difficult to effectively implement in other locations [84]. Alternately, fuel load parameters can be extracted from remote-sensing data using the inversion of radiative transfer models (RTMs) such as PROSPECT [85], SAIL [86], and GeoSail [14,87]. RTMs were developed based on physical laws that offer explicit relationships between leaf or canopy features and reflectance. Therefore, when it comes to predicting the variables of interest on a local or global scale, RTM-based techniques offer the advantage of reproducibility, making them applicable to various sensors and geographical regions [84,88]. Nonetheless, their utility is restricted by the substantial computational resources needed for model inversion. Furthermore, it is essential to incorporate prior knowledge of plant biophysical characteristics to limit the input parameters of the RTM, aligning model conditions as closely as possible with the real canopy state [89]. Additionally, the choice and configuration of the RTM are challenging, as they necessitate plant physiological and structural data that may not always be accessible, relying on assumptions that may not precisely mirror natural conditions [84,90].

Contemporary prevalent machine-learning methodologies like MLP, SVM, and RF can automatically extract patterns and relationships from the available data, allowing them to potentially adapt and provide utility across different temporal and spatial scales. Also, ML models are designed to learn patterns and relationships from data. They can handle complex relationships and adapt to different data distributions [91,92]. Training the models with data from satellite observations and field measurements is a crucial step in applying these approaches. However, to prevent underfitting issues that significantly reduce method robustness, having enough samples is necessary during the training procedure. In order to tackle this issue, previous studies have connected RTMs with machine-learning techniques. As previously stated, physics-based models leverage the principles of physics to accurately simulate interactions between light and vegetation, leading to enhanced accuracy in vegetation attributes. Consequently, these detailed attributes could serve as effective training data for machine-learning models to predict input parameters [93,94]. However, it is worth noting that these models have not seen widespread adoption for fuel load monitoring [14]. We hypothesize that the limited adoption may be attributed to the complexity of configuring these models, the availability of accessible vegetation structural data for retrieving fuel load, and the substantial computational resources required for model inversion. Advanced deep-learning (DL) techniques have been introduced and widely adopted in recent years to address challenges related to remote-sensing and geoscientific data [95–97]. These approaches for parameter retrieval exhibit remarkable efficiency, capable of processing extensive datasets while effectively accommodating the temporal and spatial characteris-

tics of the data. DL methods possess the capability to automatically extract abstract and invariant features, thus handling issues related to data dimensionality when fitting models with numerous predictors [98,99]. Consequently, the development of novel and robust DL methodologies holds the potential to enhance estimations of fuel load metrics, and research on various cutting-edge techniques is steadily expanding. Nevertheless, obstacles remain in obtaining sufficient data for algorithm calibration and validation, as well as in attaining the desired levels of precision for surface fuels.

4.2. Sensor Data Challenges

As previously described, the literature has utilized both passive (mainly optical sensors) and active (RADAR/LiDAR) remote-sensing sensors in fuel metric estimations, However, it is important to note that each type of data has its advantages and disadvantages, which are summarized in Table 5. Optical remote-sensing data records the spectral reflectance of the forest canopy, providing a two-dimensional representation of the fuel load distribution. These data often give insights into the biochemical characteristics of leaves and can provide an integrated value of all forest layers, particularly when canopy cover is sparse, though they are constrained by their inability to effectively penetrate dense canopies. Its lower sensitivity to the vertical structure of forests—a critical factor influencing fuel load distribution—can impact the accuracy of fuel load estimates, especially in forests with complex vertical structures where fuel distribution varies significantly across layers and heights [64]. In contrast, LiDAR presents significant opportunities for mapping fuel load. LiDAR has proven to be highly effective in a variety of forest applications because it enables a detailed characterization of the vegetation's vertical structure including height estimation and surface fuels [24,100]. Small-footprint airborne discrete systems, which digitize the return pulse into a small number of three-dimensional coordinates typically coinciding with the return of the first and last energy components and some intermediate energy peaks, are the most prevalent type of LiDAR systems available to resource managers [101]. These LiDAR sensors' small footprint makes the data extremely ideal for predicting and mapping fuel map features for fine-scale fire behavior and growth simulations [102]. Thus, a variety of fuel parameters, including crown dimension (CD), CH, CBD, CBH, and canopy fuel load (CFL), have been retrieved using LiDAR [24,103]. However, the extent of information retrieval from different vegetation layers varies based on the specific characteristics of the active sensors employed [104,105].

When it comes to characterizing the fuel load from various vegetation layers, discrete LiDAR systems have limitations in providing comprehensive information along the entire path traveled by the emitted pulse. On the other hand, full-waveform LiDAR systems can record the full return backscattered signal over time, offering a more detailed view of the vegetation structure and its constituents for fuel load estimations [24,106]. Thus, researchers should possess the capability to provide more comprehensive explanations of the physical characteristics of intercepted objects by analysis of the returned waveform. This is due to the fact that the waveform's amplitude at any height is proportionate to the quantity of reflective material intercepted at that height, the reflectance properties of that material, and its orientation [107]. The majority of research on fuel load characterization with LiDAR data has been conducted using airborne sensors, typically focusing on small geographic areas and fine spatial scales. However, the cost of LiDAR data acquisition restricts their temporal coverage which can hinder the analysis of fuel dynamics. Moreover, to develop effective decision-making processes for fire management, it is essential to have information on fuels at various geographical scales [79]. The potential of spaceborne LiDAR sensors such as the Global Ecosystem Dynamics Investigation (GEDI) [77], ICESat/GLAS [108], or ICESat-2/ATLAS [109] has also been demonstrated for estimating

fuel load properties. These sensors provide dense sampling of terrestrial ecosystems but not continuous coverage. Therefore, methodologies for integrating LiDAR and other satellite sensors can be developed to offer large-scale estimations of fuel load characteristics, either by extrapolating from airborne LiDAR-based estimations or by using satellite LiDAR sensors to cover broader geographical areas. For example, Leite, et al. [77] assessed GEDI's capability for estimating large-scale, multi-layer fuel loads in the Brazilian tropical savanna (Cerrado). GEDI's ability to penetrate dense vegetation is a key differentiator from previous spaceborne LiDAR sensors, such as those designed primarily for ice sheet measurements. Furthermore, GEDI features footprints separated by 60 m along track and 600 m across track—an improvement over GLAS's 70 m footprints, which were separated by approximately 170 m along the track. These enhanced technical specifications make GEDI more suitable than any prior spaceborne sensor for measuring forest structure and fuel attributes, including fuel load, at regional and global scales across various fuel types and layers.

RADAR measurements are highly sensitive to moisture content as well as crown and stem biomass, making them direct indicators of vegetation structure and biomass, especially at low frequencies (400–1500 MHz) [110]. When integrated with available allometric equations for various vegetation types, RADAR interferometric measurements can also provide vegetation height which can be easily converted to fuel load [111]. One significant advantage of RADAR remote sensing is its insensitivity to visibility conditions, allowing it to be efficiently used in situations with cloud and smoke cover, vegetation canopy obstruction, or even during day and night. Consequently, both airborne and spaceborne RADAR remote sensing have become crucial tools for monitoring and managing wildfires at a local and global scale [63]. Thus, integrating RADAR data with optical data can help to address the issue of optical imagery, such as its inability to penetrate cloud cover and dense vegetation canopy. This integration has the potential to significantly enhance the accuracy of fuel load estimations.

Thermal remote sensing also offers potential for fuel load estimation, though its application has received less attention compared to optical, LiDAR, and RADAR technologies. Thermal sensors detect emitted radiation in the thermal infrared spectrum, providing information on the surface temperature and thermal properties of vegetation [112]. These data can be particularly useful for estimating fuel moisture content, which is a critical component of fire behavior prediction [113]. Thermal imagery can detect variations in canopy temperature that may indicate differences in vegetation density and structure, potentially correlating with fuel load. Additionally, thermal data can help to identify areas of high biomass or dense vegetation, which often have lower surface temperatures due to increased evapotranspiration or shading. While no studies specifically focusing on direct fuel load estimation using thermal remote sensing were identified during this review, the technology's integration with other remote-sensing products holds promise for enhancing fuel load mapping. Future research could explore combining thermal data with other remote-sensing technologies and modeling approaches such as advanced machine-learning methods, as discussed in the methodological challenges, to address existing gaps and improve estimation accuracy.

Table 5. The benefits and drawbacks of different remote-sensing data implemented to fuel load estimation.

Remote-Sensing Sensors	Type of Data	Advantages	Disadvantages
Passive	Optical	• Sensors analyze canopy fuel load and other critical attributes in shaping fuel load. • Sensors enable differentiation of vegetation types and health conditions, which enhances the accuracy of fuel load estimation by providing insights into the vegetation composition, moisture content, etc. • The frequent revisit capabilities of many optical satellites enable regular monitoring of fuel load changes over time, essential for understanding seasonal variations, tracking accumulation rates, and identifying areas of rapid fuel build-up. • Sensors demonstrate a degree of penetration through canopies, particularly in cases where canopy coverage is not continuous, allowing for the detection of understory vegetation and surface fuels that contribute to the total fuel load. • High-resolution optical data allow for detailed analysis of vegetation patterns and fuel load distribution. • Thermal sensors provide data on surface temperature and vegetation properties, helping to detect variations in canopy temperature, identify areas of high biomass, and correlate vegetation density with fuel load.	• Dense canopies penetration limitations: lack the ability to discern whether the detected signal originates from the canopy, understory, or ground, thereby impacting fuel load estimations. • Mixed pixels can complicate accurate fuel load estimation. • Optical data provide spectral information, which is an indirect measure of fuel load. Converting spectral signatures to actual biomass quantities requires accurate modeling and extensive ground validation. • Atmospheric conditions such cloud cover and thick smoke limit their availability. • In areas with high fuel loads, optical sensors can experience signal saturation, limiting their ability to differentiate between varying levels of high fuel load. • Changes in vegetation phenology can significantly affect spectral signatures, potentially leading to inconsistent fuel load estimates across seasons.
	Thermal		

Table 5. *Cont.*

Remote-Sensing Sensors	Type of Data	Advantages	Disadvantages
Active	LiDAR	• Sensors analyze canopy and surface structural metrics which directly contribute to fuel load estimations. • Sensors provide three-dimensional information on vegetation structure, which is crucial for accurate fuel load estimation from different layers. • Sensors are able to estimate vegetation height, which is useful for a better understanding of vegetation structure, estimating the potential for ladder fuels and fuel load distribution. • Terrestrial LiDAR captures detailed ground-level data, revealing understory vegetation often overlooked by aerial or satellite LiDAR, thus providing critical information for accurately assessing understory fuel load. • High-density airborne LiDAR enables detailed mapping of fuel load variability at fine spatial scales. • Spaceborne LiDAR provides information on fuel load at large scales	• Airborne and terrestrial LiDAR typically covers limited geographic areas due to cost and logistical constraints, making large-scale fuel load mapping challenging. • Spaceborne LiDAR provides sampling rather than continuous coverage, requiring interpolation for comprehensive fuel load mapping. • Airborne and Spaceborne LiDAR systems cannot retrieve very detailed fine surface fuel load properties. • Terrestrial LiDAR data are collected from specific locations, resulting in limited coverage in fuel load estimation. • Fuel load estimates can vary based on LiDAR sensor specifications (e.g., point density, footprint size), necessitating careful calibration and validation.
	RADAR	• RADAR can penetrate vegetation canopies to varying degrees, allowing for estimation of both canopy and surface fuel load attributes. • RADAR backscatter responds to vegetation structure, enabling the estimation of key fuel load parameters such as height, fuel weight and bulk density. • It is insensitive to visibility conditions, allowing for consistent fuel load monitoring regardless of cloud cover or smoke. • Spaceborne RADAR can cover extensive areas, facilitating fuel load mapping at regional to global scales. • It is sensitive to vegetation moisture content, which is crucial for estimating available fuel load and fire behavior prediction.	• High-resolution airborne RADAR surveys for detailed fuel load mapping can be costly, limiting frequent acquisitions. • Only RADAR sensors with longer wavelengths have significant potential for fuel load estimation, particularly in dense forest environments. • Satellite RADAR can become insensitive to variations in fuel load at high levels of biomass, limiting its effectiveness in dense forest areas. • RADAR provides indirect measurements of fuel load, requiring accurate models and often ground validation to translate backscatter to meaningful fuel load estimates. • While effective for canopy and larger fuel components, RADAR may have limitations in directly measuring fine surface fuels critical for fire ignition and spread.

5. Implications and Future Directions

The diverse remote-sensing techniques used in recent years to assess fuel load are evaluated in this comprehensive review. The central focus of the paper was directed towards elucidating the remote-sensing technologies employed to quantify fuel load across distinct fuel categories from different fuel layers. The prevailing techniques for each study were encompassed, accompanied by instances of ongoing research. The discerned limitations within the scrutinized studies can be largely attributed to the inherent constraints of the existing remote-sensing technologies. The task of accurately estimating fuel load, particularly concerning surface fuel layers, poses challenges, and relying solely on one single remote-sensing data source might not invariably yield an all-encompassing approach to characterizing fuel load. Exploring innovative avenues for fuel load estimation, aligned with the capabilities and restrictions of contemporary technology, is conceivable through the possession of remote-sensing techniques that are continually advancing. Consequently, important advancements in how we use remote-sensing technology and the projected advancements in sensor technology such as upcoming optical and RADAR missions with higher spatial and temporal resolutions offer promising prospects for the evolution of detailed fuel load mapping at fine scales. Additionally, integrating emerging technologies like photogrammetry and unmanned aerial vehicles (UAVs) with optical and LiDAR technology offers the potential for highly precise fuel load mapping at sub-meter scales. Moreover, future research efforts are poised to enhance existing methodologies by incorporating advanced modeling approaches, including sophisticated machine-learning algorithms and fusion modeling techniques, to achieve the accurate analysis and prediction of fuel load dynamics. It is important to recognize that, in addition to fuel load—a key component of vegetation characterization and fire behavior models measurable through remote sensing—vegetation structural characteristics, both vertical and horizontal (e.g., height, canopy cover, plant area, and density), are also critical. These structural metrics are often easier to extract and provide valuable insights into the spatial and temporal dynamics of ecosystem functionality and fire behavior. Future research should focus on integrating fuel load estimation with vegetation structural metrics, leveraging the complementary capabilities of various remote-sensing modalities to develop a holistic understanding of vegetation dynamics and fire risk.

Author Contributions: Conceptualization, A.A. and M.Y.; conduction of primary literature review, summarization of relevant research articles, and identification of key themes and findings, A.A.; writing—original draft preparation and editing, A.A.; writing—revision and improvement, M.Y.; supervision and securing funding, M.Y. All authors have read and agreed to the published version of the manuscript.

Funding: This study was supported by funding from the Australian Research Data Commons (ARDC).

Acknowledgments: We express our gratitude to Geoff Cary, an expert in bushfire science at the Fenner School of Environment & Society, Australian National University (ANU). His valuable comments and verification of fire ecology statements greatly enhanced the quality of this manuscript.

Conflicts of Interest: The authors declare no conflicts of interest.

References

1. Mooney, H. Fire Regimes and Ecosystem Properties: Proceedings of the Conference: December 11-15, 1978, Honolulu, Hawaii. In *United States. Forest Service. USDA Forest Service General Technical Report WO (USA). No. 26*; Food and Agriculture Organization: Rome, Italy, 1981.
2. Flannigan, M.D.; Stocks, B.J.; Wotton, B.M. Climate change and forest fires. *Sci. Total Environ.* **2000**, *262*, 221–229. [CrossRef]
3. Pausas, J.G.; Keeley, J.E. Wildfires as an ecosystem service. *Front. Ecol. Environ.* **2019**, *17*, 289–295. [CrossRef]

4. Jhariya, M.K.; Raj, A. Effects of wildfires on flora, fauna and physico-chemical properties of soil-An overview. *J. Appl. Nat. Sci.* **2014**, *6*, 887–897. [CrossRef]
5. Bowman, D.M.; Moreira-Muñoz, A.; Kolden, C.A.; Chávez, R.O.; Muñoz, A.A.; Salinas, F.; González-Reyes, Á.; Rocco, R.; de la Barrera, F.; Williamson, G.J. Human–environmental drivers and impacts of the globally extreme 2017 Chilean fires. *Ambio* **2019**, *48*, 350–362. [CrossRef] [PubMed]
6. Carmona-Moreno, C.; Belward, A.; Malingreau, J.P.; Hartley, A.; Garcia-Alegre, M.; Antonovskiy, M.; Buchshtaber, V.; Pivovarov, V. Characterizing interannual variations in global fire calendar using data from Earth observing satellites. *Glob. Change Biol.* **2005**, *11*, 1537–1555. [CrossRef]
7. Jolly, W.M.; Cochrane, M.A.; Freeborn, P.H.; Holden, Z.A.; Brown, T.J.; Williamson, G.J.; Bowman, D.M. Climate-induced variations in global wildfire danger from 1979 to 2013. *Nat. Commun.* **2015**, *6*, 7537. [CrossRef] [PubMed]
8. Chuvieco, E.; Yebra, M.; Martino, S.; Thonicke, K.; Gómez-Giménez, M.; San-Miguel, J.; Oom, D.; Velea, R.; Mouillot, F.; Molina, J.R. Towards an integrated approach to wildfire risk assessment: When, where, what and how may the landscapes burn. *Fire* **2023**, *6*, 215. [CrossRef]
9. Chuvieco, E.; Riaño, D.; Aguado, I.; Cocero, D. Estimation of fuel moisture content from multitemporal analysis of Landsat Thematic Mapper reflectance data: Applications in fire danger assessment. *Int. J. Remote Sens.* **2002**, *23*, 2145–2162. [CrossRef]
10. Countryman, C.M. *The Fire Environment Concept*; Pacific Southwest Forest and Range Experiment Station: Albany, CA, USA, 1972.
11. Andrews, P.L. *BehavePlus Fire Modeling System, Version 5.0: Variables. Gen. Tech. Rep. RMRS-GTR-213 Revised*; Department of Agriculture, Forest Service, Rocky Mountain Research Station: Fort Collins, CO, USA, 2009; 111p.
12. Finney, M.A. *FARSITE, Fire Area Simulator—Model Development and Evaluation*; US Department of Agriculture, Forest Service, Rocky Mountain Research Station: Fort Collins, CO, USA, 1998.
13. Yebra, M.; Quan, X.; Riaño, D.; Larraondo, P.R.; van Dijk, A.I.; Cary, G.J. A fuel moisture content and flammability monitoring methodology for continental Australia based on optical remote sensing. *Remote Sens. Environ.* **2018**, *212*, 260–272. [CrossRef]
14. Quan, X.; Li, Y.; He, B.; Cary, G.J.; Lai, G. Application of Landsat ETM+ and OLI Data for Foliage Fuel Load Monitoring Using Radiative Transfer Model and Machine Learning Method. *IEEE J. Sel. Top. Appl. Earth Obs. Remote Sens.* **2021**, *14*, 5100–5110. [CrossRef]
15. Fernandes, P.M.; Botelho, H.S. A review of prescribed burning effectiveness in fire hazard reduction. *Int. J. Wildland fire* **2003**, *12*, 117–128. [CrossRef]
16. Alexander, M.E.; Cruz, M.G. Evaluating a model for predicting active crown fire rate of spread using wildfire observations. *Can. J. For. Res.* **2006**, *36*, 3015–3028. [CrossRef]
17. Viegas, D.; Soares, J.; Almeida, M. Combustibility of a mixture of live and dead fuel components. *Int. J. Wildland Fire* **2013**, *22*, 992–1002. [CrossRef]
18. Miller, C.; Urban, D.L. Connectivity of forest fuels and surface fire regimes. *Landsc. Ecol.* **2000**, *15*, 145–154. [CrossRef]
19. AIDR. Australian Disaster Resilience Glossary. 2022. Available online: https://knowledge.aidr.org.au/glossary (accessed on 6 February 2024).
20. Alonso-Rego, C.; Arellano-Pérez, S.; Cabo, C.; Ordoñez, C.; Álvarez-González, J.G.; Díaz-Varela, R.A.; Ruiz-González, A.D. Estimating fuel loads and structural characteristics of shrub communities by using terrestrial laser scanning. *Remote Sens.* **2020**, *12*, 3704. [CrossRef]
21. Jakubowksi, M.K.; Guo, Q.; Collins, B.; Stephens, S.; Kelly, M. Predicting surface fuel models and fuel metrics using Lidar and CIR imagery in a dense, mountainous forest. *Photogramm. Eng. Remote Sens.* **2013**, *79*, 37–49. [CrossRef]
22. Rothermel, R.C. *A Mathematical Model for Predicting Fire Spread in Wildland Fuels*; Intermountain Forest & Range Experiment Station, Forest Service, US: Fort Collins, CO, USA, 1972; Volume 115.
23. Ottmar, R.D.; Sandberg, D.V.; Riccardi, C.L.; Prichard, S.J. An overview of the fuel characteristic classification system—Quantifying, classifying, and creating fuelbeds for resource planning. *Can. J. For. Res.* **2007**, *37*, 2383–2393. [CrossRef]
24. Hermosilla, T.; Ruiz, L.A.; Kazakova, A.N.; Coops, N.C.; Moskal, L.M. Estimation of forest structure and canopy fuel parameters from small-footprint full-waveform LiDAR data. *Int. J. Wildland Fire* **2013**, *23*, 224–233. [CrossRef]
25. Lopes Queiroz, G.; McDermid, G.J.; Castilla, G.; Linke, J.; Rahman, M.M. Mapping coarse woody debris with random forest classification of centimetric aerial imagery. *Forests* **2019**, *10*, 471. [CrossRef]
26. Agee, J.; Wakimoto, R.; Darley, E.; Biswell, H. Eucalyptus fuel dynamics, and fire hazard in the Oakland Hills. *Calif. Agric.* **1973**, *27*, 13–15.
27. Olson, J.S. Energy storage and the balance of producers and decomposers in ecological systems. *Ecology* **1963**, *44*, 322–331. [CrossRef]
28. Gill, A.M. Eucalypts and fires: Interdependent or independent. In *Eucalypt Ecology: Individuals to Ecosystems*; Cambridge University Press: Cambridge, UK, 1997; pp. 151–167.
29. Gould, J.S.; McCaw, W.L.; Cheney, N.P. Quantifying fine fuel dynamics and structure in dry eucalypt forest (Eucalyptus marginata) in Western Australia for fire management. *For. Ecol. Manag.* **2011**, *262*, 531–546. [CrossRef]

30. Raison, R.; Woods, P.; Khanna, P. Decomposition and accumulation of litter after fire in sub-alpine eucalypt forests. *Aust. J. Ecol.* **1986**, *11*, 9–19. [CrossRef]
31. Murphy, B.P.; Russell-Smith, J. Fire severity in a northern Australian savanna landscape: The importance of time since previous fire. *Int. J. Wildland Fire* **2010**, *19*, 46–51. [CrossRef]
32. Keifer, M.; van Wagtendonk, J.W.; Buhler, M. Long-term surface fuel accumulation in burned and unburned mixed-conifer forests of the central and southern Sierra Nevada, CA (USA). *Fire Ecol.* **2006**, *2*, 53–72. [CrossRef]
33. Bresnehan, S.J. An Assessment of Fuel Characteristics and Fuel Loads in the Dry Sclerophyll Forests of South-East Tasmania. Ph.D. Thesis, University of Tasmania, Sydney, Australia, 2003.
34. Gilroy, J.; Tran, C. A new fuel load model for eucalypt forests in southeast Queensland. *Proc. R. Soc. Qld.* **2009**, *115*, 137–143. [CrossRef]
35. Rollins, M.G.; Keane, R.E.; Parsons, R.A. Mapping fuels and fire regimes using remote sensing, ecosystem simulation, and gradient modeling. *Ecol. Appl.* **2004**, *14*, 75–95. [CrossRef]
36. Zhang, R.; Zhou, X.; Ouyang, Z.; Avitabile, V.; Qi, J.; Chen, J.; Giannico, V. Estimating aboveground biomass in subtropical forests of China by integrating multisource remote sensing and ground data. *Remote Sens. Environ.* **2019**, *232*, 111341. [CrossRef]
37. Forkuor, G.; Zoungrana, J.-B.B.; Dimobe, K.; Ouattara, B.; Vadrevu, K.P.; Tondoh, J.E. Above-ground biomass mapping in West African dryland forest using Sentinel-1 and 2 datasets-A case study. *Remote Sens. Environ.* **2020**, *236*, 111496. [CrossRef]
38. Gale, M.G.; Cary, G.J.; Van Dijk, A.I.; Yebra, M. Forest fire fuel through the lens of remote sensing: Review of approaches, challenges and future directions in the remote sensing of biotic determinants of fire behaviour. *Remote Sens. Environ.* **2021**, *255*, 112282. [CrossRef]
39. Keane, R.E. Describing wildland surface fuel loading for fire management: A review of approaches, methods and systems. *Int. J. Wildland Fire* **2012**, *22*, 51–62. [CrossRef]
40. Franke, J.; Barradas, A.C.S.; Borges, M.A.; Costa, M.M.; Dias, P.A.; Hoffmann, A.A.; Orozco Filho, J.C.; Melchiori, A.E.; Siegert, F. Fuel load mapping in the Brazilian Cerrado in support of integrated fire management. *Remote Sens. Environ.* **2018**, *217*, 221–232. [CrossRef]
41. Cruz, M.G.; Alexander, M.E.; Wakimoto, R.H. Assessing canopy fuel stratum characteristics in crown fire prone fuel types of western North America. *Int. J. Wildland Fire* **2003**, *12*, 39–50. [CrossRef]
42. Wagner, C.V. Conditions for the start and spread of crown fire. *Can. J. For. Res.* **1977**, *7*, 23–34. [CrossRef]
43. Scott, J.H. *Assessing Crown Fire Potential by Linking Models of Surface and Crown Fire Behavior*; US Department of Agriculture, Forest Service, Rocky Mountain Research Station: Fort Collins, CO, USA, 2001.
44. Chuvieco, E.; Riaño, D.; Van Wagtendok, J.; Morsdof, F. Fuel loads and fuel type mapping. In *Wildland Fire Danger Estimation and Mapping: The Role of Remote Sensing data*; World Scientific: Singapore, 2003; pp. 119–142.
45. Andrews, P.L.; Queen, L.P. Fire modeling and information system technology. *Int. J. Wildland Fire* **2001**, *10*, 343–352. [CrossRef]
46. Reich, R.M.; Lundquist, J.E.; Bravo, V.A. Spatial models for estimating fuel loads in the Black Hills, South Dakota, USA. *Int. J. Wildland Fire* **2004**, *13*, 119–129. [CrossRef]
47. Andrews, P.L. *BEHAVE: Fire Behavior Prediction and Fuel Modeling System: BURN Subsystem, Part 1*; US Department of Agriculture, Forest Service, Intermountain Research Station: Fort Collins, CO, USA, 1986; Volume 194.
48. Ivanova, G.A.; Kukavskaya, E.A.; Ivanov, V.A.; Conard, S.G.; McRae, D.J. Fuel characteristics, loads and consumption in Scots pine forests of central Siberia. *J. For. Res.* **2020**, *31*, 2507–2524. [CrossRef]
49. Arroyo, L.A.; Pascual, C.; Manzanera, J.A. Fire models and methods to map fuel types: The role of remote sensing. *For. Ecol. Manag.* **2008**, *256*, 1239–1252. [CrossRef]
50. Sullivan, A.; Surawski, N.; Crawford, D.; Hurley, R.; Volkova, L.; Weston, C.; Meyer, C. Effect of woody debris on the rate of spread of surface fires in forest fuels in a combustion wind tunnel. *For. Ecol. Manag.* **2018**, *424*, 236–245. [CrossRef]
51. Fosberg, M.A. Drying rates of heartwood below fiber saturation. *For. Sci.* **1970**, *16*, 57–63.
52. Falkowski, M.J.; Gessler, P.E.; Morgan, P.; Hudak, A.T.; Smith, A.M. Characterizing and mapping forest fire fuels using ASTER imagery and gradient modeling. *For. Ecol. Manag.* **2005**, *217*, 129–146. [CrossRef]
53. Massetti, A.; Rüdiger, C.; Yebra, M.; Hilton, J. The Vegetation Structure Perpendicular Index (VSPI): A forest condition index for wildfire predictions. *Remote Sens. Environ.* **2019**, *224*, 167–181. [CrossRef]
54. Jin, S.; Chen, S.-C. Application of QuickBird imagery in fuel load estimation in the Daxinganling region, China. *Int. J. Wildland Fire* **2012**, *21*, 583–590. [CrossRef]
55. Arellano-Pérez, S.; Castedo-Dorado, F.; López-Sánchez, C.A.; González-Ferreiro, E.; Yang, Z.; Díaz-Varela, R.A.; Álvarez-González, J.G.; Vega, J.A.; Ruiz-González, A.D. Potential of sentinel-2A data to model surface and canopy fuel characteristics in relation to crown fire hazard. *Remote Sens.* **2018**, *10*, 1645. [CrossRef]
56. Oliveira, U.; Soares-Filho, B.; de Souza Costa, W.L.; Gomes, L.; Bustamante, M.; Miranda, H. Modeling fuel loads dynamics and fire spread probability in the Brazilian Cerrado. *For. Ecol. Manag.* **2021**, *482*, 118889. [CrossRef]

57. Wells, A.G.; Munson, S.M.; Sesnie, S.E.; Villarreal, M.L. Remotely Sensed Fine-Fuel Changes from Wildfire and Prescribed Fire in a Semi-Arid Grassland. *Fire* **2021**, *4*, 84. [CrossRef]
58. Chaivaranont, W. How Does Remotely Sensed Degree of Curing and Fuel Load Vary in Grasslands and Effect Modelled Fire Spread? Ph.D. Thesis, UNSW Sydney, Sydney, Australia, 2018.
59. Skowronski, N.S.; Clark, K.L.; Duveneck, M.; Hom, J. Three-dimensional canopy fuel loading predicted using upward and downward sensing LiDAR systems. *Remote Sens. Environ.* **2011**, *115*, 703–714. [CrossRef]
60. Clark, K.L.; Skowronski, N.; Gallagher, M.; Carlo, N.; Farrell, M.; Maghirang, M.R. *Assessment of Canopy Fuel Loading Across a Heterogeneous Landscape Using LiDAR*; USDA Forest Service: Fort Collins, CO, USA, 2010.
61. Bai, X.; He, B.; Li, X.; Zeng, J.; Wang, X.; Wang, Z.; Zeng, Y.; Su, Z. First assessment of Sentinel-1A data for surface soil moisture estimations using a coupled water cloud model and advanced integral equation model over the Tibetan Plateau. *Remote Sens.* **2017**, *9*, 714. [CrossRef]
62. Wang, L.; Quan, X.; He, B.; Yebra, M.; Xing, M.; Liu, X. Assessment of the dual polarimetric sentinel-1A data for forest fuel moisture content estimation. *Remote Sens.* **2019**, *11*, 1568. [CrossRef]
63. Saatchi, S.; Halligan, K.; Despain, D.G.; Crabtree, R.L. Estimation of forest fuel load from radar remote sensing. *IEEE Trans. Geosci. Remote Sens.* **2007**, *45*, 1726–1740. [CrossRef]
64. Li, Y.; Quan, X.; Liao, Z.; He, B. Forest Fuel Loads Estimation from Landsat ETM+ and ALOS PALSAR Data. *Remote Sens.* **2021**, *13*, 1189. [CrossRef]
65. Debastiani, A.B.; Sanquetta, C.R.; Dalla Corte, A.P.; Pinto, N.S.; Rex, F.E. Evaluating SAR-optical sensor fusion for aboveground biomass estimation in a Brazilian tropical forest. *Ann. For. Res.* **2019**, *62*, 109–122. [CrossRef]
66. Nuthammachot, N.; Askar, A.; Stratoulias, D.; Wicaksono, P. Combined use of Sentinel-1 and Sentinel-2 data for improving above-ground biomass estimation. *Geocarto Int.* **2022**, *37*, 366–376. [CrossRef]
67. Cho, M.A.; Mathieu, R.; Asner, G.P.; Naidoo, L.; Van Aardt, J.; Ramoelo, A.; Debba, P.; Wessels, K.; Main, R.; Smit, I.P. Mapping tree species composition in South African savannas using an integrated airborne spectral and LiDAR system. *Remote Sens. Environ.* **2012**, *125*, 214–226. [CrossRef]
68. Chen, Y.; Zhu, X.; Yebra, M.; Harris, S.; Tapper, N. Development of a predictive model for estimating forest surface fuel load in Australian eucalypt forests with LiDAR data. *Environ. Model. Softw.* **2017**, *97*, 61–71. [CrossRef]
69. Cameron, H.; Schroeder, D.; Beverly, J. Predicting black spruce fuel characteristics with Airborne Laser Scanning (ALS). *Int. J. Wildland Fire* **2021**, *31*, 124–135. [CrossRef]
70. Stefanidou, A.; Gitas, I.Z.; Korhonen, L.; Georgopoulos, N.; Stavrakoudis, D. Multispectral lidar-based estimation of surface fuel load in a dense coniferous forest. *Remote Sens.* **2020**, *12*, 3333. [CrossRef]
71. Price, O.F.; Gordon, C.E. The potential for LiDAR technology to map fire fuel hazard over large areas of Australian forest. *J. Environ. Manag.* **2016**, *181*, 663–673. [CrossRef]
72. Lin, C.; Ma, S.-E.; Huang, L.-P.; Chen, C.-I.; Lin, P.-T.; Yang, Z.-K.; Lin, K.-T. Generating a Baseline Map of Surface Fuel Loading Using Stratified Random Sampling Inventory Data through Cokriging and Multiple Linear Regression Methods. *Remote Sens.* **2021**, *13*, 1561. [CrossRef]
73. McCarley, T.R.; Hudak, A.T.; Restaino, J.C.; Billmire, M.; French, N.H.; Ottmar, R.D.; Hass, B.; Zarzana, K.; Goulden, T.; Volkamer, R. A comparison of multitemporal airborne laser scanning data and the Fuel Characteristics Classification System for estimating fuel load and consumption. *J. Geophys. Res. Biogeosci.* **2022**, *127*, e2021JG006733. [CrossRef]
74. González-Ferreiro, E.; Arellano-Pérez, S.; Castedo-Dorado, F.; Hevia, A.; Vega, J.A.; Vega-Nieva, D.; Álvarez-González, J.G.; Ruiz-González, A.D. Modelling the vertical distribution of canopy fuel load using national forest inventory and low-density airbone laser scanning data. *PLoS ONE* **2017**, *12*, e0176114. [CrossRef] [PubMed]
75. Alonso-Rego, C.; Arellano-Pérez, S.; Guerra-Hernández, J.; Molina-Valero, J.A.; Martínez-Calvo, A.; Pérez-Cruzado, C.; Castedo-Dorado, F.; González-Ferreiro, E.; Álvarez-González, J.G.; Ruiz-González, A.D. Estimating Stand and Fire-Related Surface and Canopy Fuel Variables in Pine Stands Using Low-Density Airborne and Single-Scan Terrestrial Laser Scanning Data. *Remote Sens.* **2021**, *13*, 5170. [CrossRef]
76. Marselis, S.M.; Yebra, M.; Jovanovic, T.; van Dijk, A.I. Deriving comprehensive forest structure information from mobile laser scanning observations using automated point cloud classification. *Environ. Model. Softw.* **2016**, *82*, 142–151. [CrossRef]
77. Leite, R.V.; Silva, C.A.; Broadbent, E.N.; Do Amaral, C.H.; Liesenberg, V.; De Almeida, D.R.A.; Mohan, M.; Godinho, S.; Cardil, A.; Hamamura, C. Large scale multi-layer fuel load characterization in tropical savanna using GEDI spaceborne lidar data. *Remote Sens. Environ.* **2022**, *268*, 112764. [CrossRef]
78. Myroniuk, V.; Zibtsev, S.; Bogomolov, V.; Goldammer, J.G.; Soshenskyi, O.; Levchenko, V.; Matsala, M. Combining Landsat time series and GEDI data for improved characterization of fuel types and canopy metrics in wildfire simulation. *J. Environ. Manag.* **2023**, *345*, 118736. [CrossRef]
79. García, M.; Saatchi, S.; Casas, A.; Koltunov, A.; Ustin, S.L.; Ramirez, C.; Balzter, H. Extrapolating forest canopy fuel properties in the California Rim Fire by combining airborne LiDAR and Landsat OLI data. *Remote Sens.* **2017**, *9*, 394. [CrossRef]

80. Erdody, T.L.; Moskal, L.M. Fusion of LiDAR and imagery for estimating forest canopy fuels. *Remote Sens. Environ.* **2010**, *114*, 725–737. [CrossRef]
81. Skowronski, N.S.; Haag, S.; Trimble, J.; Clark, K.L.; Gallagher, M.R.; Lathrop, R.G. Structure-level fuel load assessment in the wildland–urban interface: A fusion of airborne laser scanning and spectral remote-sensing methodologies. *Int. J. Wildland Fire* **2015**, *25*, 547–557. [CrossRef]
82. Li, Y.; He, B.; Kong, P.; Xu, H.; Zhang, Q.; Quan, X. Estimation of Forest Surface Dead Fuel Loads Based on Multi-Source Remote Sensing Data. In Proceedings of the 2021 IEEE International Geoscience and Remote Sensing Symposium IGARSS, Brussels, Belgium, 11–16 July 2021; pp. 6893–6896.
83. D'Este, M.; Elia, M.; Giannico, V.; Spano, G.; Lafortezza, R.; Sanesi, G. Machine learning techniques for fine dead fuel load estimation using multi-source remote sensing data. *Remote Sens.* **2021**, *13*, 1658. [CrossRef]
84. Yebra, M.; Dennison, P.E.; Chuvieco, E.; Riaño, D.; Zylstra, P.; Hunt, E.R., Jr.; Danson, F.M.; Qi, Y.; Jurdao, S. A global review of remote sensing of live fuel moisture content for fire danger assessment: Moving towards operational products. *Remote Sens. Environ.* **2013**, *136*, 455–468. [CrossRef]
85. Feret, J.-B.; François, C.; Asner, G.P.; Gitelson, A.A.; Martin, R.E.; Bidel, L.P.; Ustin, S.L.; Le Maire, G.; Jacquemoud, S. PROSPECT-4 and 5: Advances in the leaf optical properties model separating photosynthetic pigments. *Remote Sens. Environ.* **2008**, *112*, 3030–3043. [CrossRef]
86. Verhoef, W. Theory of Radiative Transfer Models Applied in Optical Remote Sensing of Vegetation Canopies. Ph.D. Thesis, Wageningen University and Research, Wageningen, The Netherlands, 1998.
87. Verhoef, W. Light scattering by leaf layers with application to canopy reflectance modeling: The SAIL model. *Remote Sens. Environ.* **1984**, *16*, 125–141. [CrossRef]
88. Bowyer, P.; Danson, F. Sensitivity of spectral reflectance to variation in live fuel moisture content at leaf and canopy level. *Remote Sens. Environ.* **2004**, *92*, 297–308. [CrossRef]
89. Yebra, M.; Chuvieco, E. Linking ecological information and radiative transfer models to estimate fuel moisture content in the Mediterranean region of Spain: Solving the ill-posed inverse problem. *Remote Sens. Environ.* **2009**, *113*, 2403–2411. [CrossRef]
90. Combal, B.; Baret, F.; Weiss, M. Improving canopy variables estimation from remote sensing data by exploiting ancillary information. Case study on sugar beet canopies. *Agronomie* **2002**, *22*, 205–215. [CrossRef]
91. Zhong, L.; Hu, L.; Zhou, H. Deep learning based multi-temporal crop classification. *Remote Sens. Environ.* **2019**, *221*, 430–443. [CrossRef]
92. Abdollahi, A.; Pradhan, B.; Alamri, A. Regional-Scale Analysis of Vegetation Dynamics Using Satellite Data and Machine Learning Algorithms: A Multi-Factorial Approach. *Int. J. Smart Sens. Intell. Syst.* **2023**, *16*. [CrossRef]
93. Gewali, U.B.; Monteiro, S.T.; Saber, E. Gaussian processes for vegetation parameter estimation from hyperspectral data with limited ground truth. *Remote Sens.* **2019**, *11*, 1614. [CrossRef]
94. Svendsen, D.H.; Morales-Álvarez, P.; Ruescas, A.B.; Molina, R.; Camps-Valls, G. Deep Gaussian processes for biogeophysical parameter retrieval and model inversion. *ISPRS J. Photogramm. Remote Sens.* **2020**, *166*, 68–81. [CrossRef]
95. Camps-Valls, G.; Reichstein, M.; Zhu, X.; Tuia, D. Advancing deep learning for earth sciences: From hybrid modeling to interpretability. In Proceedings of the IGARSS 2020-2020 IEEE International Geoscience and Remote Sensing Symposium, Waikoloa, HI, USA, 26 September–2 October 2020; pp. 3979–3982.
96. Abdollahi, A.; Pradhan, B. Explainable artificial intelligence (XAI) for interpreting the contributing factors feed into the wildfire susceptibility prediction model. *Sci. Total Environ.* **2023**, *879*, 163004. [CrossRef]
97. Abdollahi, A.; Pradhan, B. Urban vegetation mapping from aerial imagery using explainable AI (XAI). *Sensors* **2021**, *21*, 4738. [CrossRef] [PubMed]
98. Zhang, L.; Shao, Z.; Liu, J.; Cheng, Q. Deep learning based retrieval of forest aboveground biomass from combined LiDAR and landsat 8 data. *Remote Sens.* **2019**, *11*, 1459. [CrossRef]
99. Abdollahi, A.; Liu, Y.; Pradhan, B.; Huete, A.; Dikshit, A.; Tran, N.N. Short-time-series grassland mapping using Sentinel-2 imagery and deep learning-based architecture. *Egypt. J. Remote Sens. Space Sci.* **2022**, *25*, 673–685. [CrossRef]
100. Van Leeuwen, M.; Nieuwenhuis, M. Retrieval of forest structural parameters using LiDAR remote sensing. *Eur. J. For. Res.* **2010**, *129*, 749–770. [CrossRef]
101. Hall, S.; Burke, I.; Box, D.; Kaufmann, M.; Stoker, J.M. Estimating stand structure using discrete-return lidar: An example from low density, fire prone ponderosa pine forests. *For. Ecol. Manag.* **2005**, *208*, 189–209. [CrossRef]
102. Keane, R.E.; Burgan, R.; van Wagtendonk, J. Mapping wildland fuels for fire management across multiple scales: Integrating remote sensing, GIS, and biophysical modeling. *Int. J. Wildland Fire* **2001**, *10*, 301–319. [CrossRef]
103. González-Olabarria, J.-R.; Rodríguez, F.; Fernández-Landa, A.; Mola-Yudego, B. Mapping fire risk in the Model Forest of Urbión (Spain) based on airborne LiDAR measurements. *For. Ecol. Manag.* **2012**, *282*, 149–156. [CrossRef]

104. Fragoso-Campón, L.; Quirós, E.; Mora, J.; Gutiérrez Gallego, J.A.; Durán-Barroso, P. Overstory-understory land cover mapping at the watershed scale: Accuracy enhancement by multitemporal remote sensing analysis and LiDAR. *Environ. Sci. Pollut. Res.* **2020**, *27*, 75–88. [CrossRef] [PubMed]
105. Mutlu, M.; Popescu, S.C.; Stripling, C.; Spencer, T. Mapping surface fuel models using lidar and multispectral data fusion for fire behavior. *Remote Sens. Environ.* **2008**, *112*, 274–285. [CrossRef]
106. Abdollahi, A.; Yebra, M. Forest fuel type classification: Review of remote sensing techniques, constraints and future trends. *J. Environ. Manag.* **2023**, *342*, 118315. [CrossRef]
107. Hyde, P.; Dubayah, R.; Peterson, B.; Blair, J.; Hofton, M.; Hunsaker, C.; Knox, R.; Walker, W. Mapping forest structure for wildlife habitat analysis using waveform lidar: Validation of montane ecosystems. *Remote Sens. Environ.* **2005**, *96*, 427–437. [CrossRef]
108. García, M.; Popescu, S.; Riaño, D.; Zhao, K.; Neuenschwander, A.; Agca, M.; Chuvieco, E. Characterization of canopy fuels using ICESat/GLAS data. *Remote Sens. Environ.* **2012**, *123*, 81–89. [CrossRef]
109. Gwenzi, D.; Lefsky, M.A.; Suchdeo, V.P.; Harding, D.J. Prospects of the ICESat-2 laser altimetry mission for savanna ecosystem structural studies based on airborne simulation data. *ISPRS J. Photogramm. Remote Sens.* **2016**, *118*, 68–82. [CrossRef]
110. Saatchi, S.S.; Moghaddam, M. Estimation of crown and stem water content and biomass of boreal forest using polarimetric SAR imagery. *IEEE Trans. Geosci. Remote Sens.* **2000**, *38*, 697–709. [CrossRef]
111. Andersen, H.-E.; McGaughey, R.; Reutebuch, S.; Schreudera, G.; Agee, J.; Mercer, B. Estimating canopy fuel parameters in a Pacific Northwest conifer forest using multifrequency polarimetric IFSAR. *Image* **2004**, *900*, 74.
112. Kumar, D.; Shekhar, S. Statistical analysis of land surface temperature–vegetation indexes relationship through thermal remote sensing. *Ecotoxicol. Environ. Saf.* **2015**, *121*, 39–44. [CrossRef] [PubMed]
113. Fan, L.; Wigneron, J.-P.; Xiao, Q.; Al-Yaari, A.; Wen, J.; Martin-StPaul, N.; Dupuy, J.-L.; Pimont, F.; Al Bitar, A.; Fernandez-Moran, R. Evaluation of microwave remote sensing for monitoring live fuel moisture content in the Mediterranean region. *Remote Sens. Environ.* **2018**, *205*, 210–223. [CrossRef]